High Resolution DEMs for Urban Applications from NAPP Photography

Curt H. Davis and Xiangyun Wang

Institute for the Commercial Development of Remote Sensing Technologies
University of Missouri-Columbia
323 Engineering Bldg. West
Department of Electrical Engineering
Columbia, MO 65211
Davisch@missouri.edu
Xiangyunw@hotmail.com

Abstract

Digital Elevation Models (DEMs) are widely used in many GIS and resource management applications. Increased use of DEMs has led to greater demand for higher resolution and higher accuracy digital elevation data. Here we demonstrate that digitally-scanned 1:40,000-scale NAPP aerial photography, used in conjunction with precision ground control, can be used to generate DEMs with horizontal resolutions of 1-3 m. The vertical accuracies of the DEMs were evaluated using more than 50,000 check points derived from a precision kinematic GPS survey. The results indicate the DEMs have RMS vertical accuracies on the order of 1.8-2.5 m.

The DEMs are shown to reveal very fine-scale features in an urban test area. The horizontal resolution and vertical accuracy of the NAPP DEMs are many times better than those currently derived from satellite remote sensing platforms. Moreover, the NAPP imagery are an inexpensive source of data that are readily available throughout most of the United States. The exploitation of the NAPP data could make high-resolution/high-accuracy DEMs available to smaller cities and counties who would otherwise be unable to afford more expensive commercial datasets of comparable resolution and accuracy.

Introduction

Digital Elevation Models (DEMs) are the digital representation of topographic and/or man-made features located on the surface of the earth. DEMs are widely used for hydrologic analyses, resource management, transportation planning, earth sciences, environmental assessment, and military applications. Increased use of DEMs in these wide-ranging applications has led to greater need for higher resolution and higher accuracy digital elevation data. This is especially true for urban applications such as base map registration, stormwater management, and flood-risk assessment because of the fine horizontal and vertical spatial scale of most urban features (streets, buildings, etc.).

There are several commonly used satellite data sources for high-resolution DEMs, and these fall into two categories: optical and radar. Stereo-correlation processing of panchromatic imagery from the SPOT satellite typically produce DEMs with a 20 m horizontal (xy) resolution. The RMS vertical (z) accuracies of SPOT DEMs can vary from about 4-5 m in low-relief areas (Rodriguez *et al.*, 1988) to over 100 m in other areas (Fukushima, 1988). However, typical absolute RMS

vertical accuracies for SPOT DEMs are on the order of 8-15 m (e.g. Sasowksy *et al.*, 1992; Al-Rousan *et al.*, 1997). DEMs available directly from SPOT Image, Inc. have a 20 m xy resolution and a 7-11 m relative RMS z accuracy (Spot Image, 2000). Similarly, DEMs produced from Interferometric Synthetic Aperture Radar (InSAR) image processing (e.g. ERS-1/2) have yielded 25 m xy resolutions and 10-30 m RMS z accuracies (e.g. Gens and Genderson, 1996; Rufino *et al.*, 1998). The recently completed Shuttle Radar Topography Mission (SRTM) used a very accurate InSAR system which will soon provide DEMs in the continental U.S. with 30 m xy resolution and a projected absolute RMS z accuracy < 10 m (NASA SRTM, 2000).

The most widely available high-resolution DEMs in the U.S. are the 7.5-minute Level 1 DEMs available from the United States Geological Survey (USGS). These are produced from 1:40,000-scale panchromatic aerial photographs acquired by the National Aerial Photography Program (NAPP) (Light, 1993) using automated stereo-correlation processing. The USGS 7.5-minute DEMs have a 30 m xy resolution, a 7-15 m RMS z accuracy, and are available for about 90% of the continental U.S (USGS, 1997). The horizontal resolution and vertical accuracy of all the DEMs described above are not suitable for the vast majority of urban applications.

Recently, this has prompted development of higher-resolution and/or higher accuracy DEM data products from commercial remote sensing data providers. These providers use airborne InSAR and LIDAR (LIght Detection And Ranging) systems for topographic mapping. For example, the Intermap STAR 3i X-band InSAR system can provide digital elevation data with a 5 m xy resolution and a 3 m RMS z accuracy (Intermap, 2000). Commercial LIDAR systems can provide 1.5 m xy resolution and 0.4 m vertical accuracy (e.g. Terrapoint Inc., 2000). However, the cost of commercial InSAR and LIDAR data is in most cases too great for widespread adoption by city and county governments in areas other than major metropolitan cities. In this paper we demonstrate that high-resolution DEMs can be derived from 1:40,000-scale NAPP aerial photographs with sufficient horizontal resolution and vertical accuracy to be useful for many urban applications. This is an important low-cost data source that is readily available throughout most of the U.S.

Datasets and Processing

Source Data

The NAPP program has acquired 1:40,000-scale photographs for about 95% of the continental U.S. and this coverage is repeated approximately every 5 years. The flight lines are quarter-quad centered on 1:24,000-scale USGS topographic maps and the photographs are acquired at 20,000 ft. (6,100 m) above mean terrain with a 6-inch focal length lens (Light, 1993). The photographs are acquired with ~60% north/south (N/S) overlap and >27% east/west (E/W) overlap. NAPP photographs are used by the USGS to produce the 30 m Level 1 DEMs noted above as well as the Digital Orthorectified Quarter Quad (DOQQ) images. Both of these products are widely used in many GIS applications. The City of Springfield, Missouri was selected as the location for this pilot study. Springfield is located in south-central Missouri and is a medium-sized city with a population of about 140,000.

Eight photographs, acquired in leaf-off conditions on November 6, 1996, were obtained from the NAPP archive. The selected photos provided coverage of about 90% of the area within the Springfield city limits. The eight photos were oriented in two adjacent N/S strips, each containing four photos. The panchromatic film positives were precision scanned by a third-party vendor to ensure the photogrammetric and geometric integrity of the images was preserved. The latter is critical for high-resolution DEM extraction, and the use of film positives rather than prints ensures the best possible geometric integrity. A scanning resolution of 21.2 μm (1200 dpi) was used to produce digital images with a corresponding pixel size of 0.85 m. The NAPP data support a scanning resolution as low as 15 μm (1690 dpi) (Light, 1993). As the images are not geo-referenced, accurate ground control data must be acquired so that the eight photos could be tied to a common coordinate reference frame.

Ground Control Data

Two different ground control datasets were used in this study. The first dataset was comprised of eleven National Geodetic Survey (NGS) monuments that were uniformly distributed throughout the study area (Figure 2). The NGS monuments were first-order horizontal benchmarks that were tied to the U.S. High Accuracy Reference Network (HARN). In addition, the Missouri Department of Natural Resources had tied these monuments to known vertical benchmarks using precision land survey methods. Both the horizontal and vertical positions have an estimated accuracy on the order of 1-2 cm. A field inspection was conducted to determine, as closely as possible, the exact pixel location of each of the NGS monuments in the corresponding digital image. For three of the eleven monuments, it was not possible to determine, with sufficient certainty, the precise pixel location. Thus, the first Ground Control Point (GCP) database contained eight of the NGS monuments. This GCP database was used in this study to generate Level 0 DEMs. The purpose of the Level 0 DEMs is to document the accuracy of the high-resolution DEMs when only a limited number of existing GCPs are available for use.

The second ground control dataset was acquired during a two-day rapid-static differential GPS survey in the study area. A total of 52 potential GCPs, uniformly distributed in the study area, were identified *a priori* in the digital images in locations with sharp and distinct point features. This is important because the accuracy of the DEM coordinate reference frame from aerial triangulation will depend on the ability to precisely locate each GCP in the corresponding digital images. With ~60% N/S and ~30% E/W overlap, the number of images a given GCP may appear in varies from a minimum of 2 to a maximum of 6. Ashtech Z-surveyor differential GPS receivers were used for the survey. These are dual-frequency (L1/L2) 12-channel differential GPS units. The GPS base unit was located on NGS monuments GR12 and GR03 (Figure 2) on the first and second survey days, respectively. The GPS rover unit occupied each static position for a period of 4-5 minutes and maintained nearly continuous tracking of the available GPS satellites between static site occupations. A maximum baseline distance (separation between base and rover units) of 8 km was allowed. In addition to occupying the GCP sites, the GPS rover unit also occupied nine of the NGS monument sites, also for a period of 4-5 minutes, to provide an external check on the absolute accuracy of the GPS-derived GCP positions.

Table 1 summarizes the comparison between the known NGS positions and the computed GPS positions for the nine monuments. The xy coordinates are NAD83 state plane and the z

coordinate is NAVD88. The results show excellent agreement between the GPS and NGS positions. The RMS of the difference between the GPS and NGS positions was 1.0, 1.2, and 2.0 cm for the x, y, and z coordinates, respectively. While the GPS points were selected *a priori* using the digital imagery, a total of 6 of the points were eventually excluded because the precise location was difficult to determine in at least one of the other images that the GCP appeared in. Thus, the second GCP database contained a total of 46 GPS points. This GCP database was used to generate Level 1 DEMs, which represent a best-case scenario in terms of the quantity and accuracy of the GCP data.

Table 1. Comparison of GPS positions at known NGS monument sites

NGS Station	NGS Positions (m)			GPS Positions (m)			Difference (cm)		
	Northing	Easting	Elev	Northing	Easting	Elev	Northing	Easting	Elev
DON	150045.51	423782.71	383.04	150045.51	423782.71	383.05	0.00	-0.60	0.40
GR06	147168.87	432226.58	402.63	147168.87	432226.57	402.64	0.00	-1.80	1.50
GR13	153351.10	432375.85	401.96	153351.12	432375.86	401.97	1.40	0.90	0.80
GR29	156609.06	424631.02	388.29	156609.07	424631.02	388.29	0.98	0.40	-0.10
GR42	152541.18	424463.25	376.73	152541.18	424463.23	376.73	-0.05	-1.55	0.30
JEFF	149863.57	432362.10	408.42	149863.55	432362.09	408.40	-1.90	-1.30	-2.10
REED	155719.41	429578.87	413.86	155719.40	429578.86	413.88	-0.28	-0.53	2.20
SMNL	149257.34	426129.02	388.40	149257.33	426129.03	388.41	-0.40	0.80	1.20
TRCK	156345.26	433117.94	412.04	156345.26	433117.93	412.09	0.55	-1.51	4.80

Calibration/Triangulation

The raw aerial photos contain geometric distortions and are not tied to a ground coordinate system. The geometric distortions can be caused by such things as earth curvature, atmospheric refraction, and camera-lens distortion to name a few. Prior to stereo-correlation processing of the images for DEM extraction, the digitized photos must be geometrically corrected and transformed into a standard cartographic projection. These steps follow standard photogrammetric procedures and are only summarized here.

Camera calibration data (fiducial coordinates, lens distortion coefficients, principal x and y offset, etc.) are available for all NAPP photos. These data are used in conjunction with manual measurements of the fiducial marks on each photo to develop an interior orientation solution. After this, GCPs are identified in all images in which they occur to develop a mathematical transformation from image space to ground coordinate space. In addition, a series of Tie Points (TPs) (unknown position) are collected to improve the relative orientation between the set of eight photos. A collection of 32 TPs and 20 TPs were used for the Level 0 and Level 1 DEM triangulation solutions, respectively. For this study, the triangulation solution provides a simultaneous estimate of the eight camera positions (i.e. 1/photo) which seeks to minimize the vector differences between the estimated camera positions and all GCPs. A total of 24 and 130 vectors were used in the Level 0 and Level 1 triangulation solutions, respectively. The solution follows an iterative least squares approach and the result provides an overall estimate of the RMS accuracy of the coordinate reference frame. For the Level 0 DEM triangulation solution, the RMS

x, y, and z accuracies were 0.64, 0.84, and 0.25 m, respectively. For the Level 1 DEM triangulation solution, the RMS x, y, and z accuracies were 0.57, 0.56, and 0.24 m, respectively.

Since the absolute accuracies of the GCP data are on the order of a few cm for all coordinates (Table 1), the triangulation errors are dominated by the uncertainty in the GCP locations in the digital images. The results above indicate that sub-pixel (< 0.85 m) coordinate accuracy was obtained for the Level 0 and Level 1 DEM solutions. The practical horizontal triangulation accuracy for the NAPP imagery is estimated to be about 0.8 m (Light, 1993). For the Level 1 DEM triangulation solution, the horizontal accuracy is $\sqrt{0.57^2 + 0.56^2} = 0.80$, and this was achieved using a scanning resolution slightly worse than that supported by the NAPP photos. The vertical accuracy of both triangulation solutions (~0.25 m) are substantially smaller than the 0.7 m theoretical vertical (z) accuracy supported by the NAPP photos (Light, 1993). However, the vertical accuracies of the DEMs will be much larger than that indicated by the triangulation solution because of imperfect stereo-correlation matching between image pairs during the DEM extraction process.

Check Point Data

A number of check-point (CP) databases were developed to assess the overall vertical accuracy of the Level 0 and Level 1 DEMs. The first check-point dataset, hereafter CP_{S50}, was made up of the 52 GPS positions from the rapid-static GPS survey. This is a reasonable dataset to assess the vertical accuracy of the Level 0 DEMs, but is insufficient for the Level 1 DEMs since most of these data were used as GCPs in that triangulation solution. The second check-point dataset, CP_{S100}, was comprised of 102 points obtained from multiple static GPS surveys conducted by the City of Springfield's survey office. The vertical accuracy of these data is estimated to be about 3 cm (J. Dill, personal communication). This estimate was obtained by comparing GPS-derived positions with NGS monument positions, just as we have done in Table 1.

Three other CP datasets were derived from kinematic GPS data collected during our two-day GPS survey. In between the rapid-static site occupations for collection of the Level 1 GCP data, the GPS rover unit collected kinematic data at a rate of 5 or 10 Hz, where the GPS antenna was magnetically mounted on the survey vehicle. The kinematic GPS data therefore enable the collection of a large number of densely spaced CPs, even when traveling at high rates of speed. For example, at 45 mph the ground spacing between CPs is 4 m for a 5 Hz sampling rate. The accuracy of the kinematic GPS data will be worse than that of the rapid-static GPS data for two reasons. First, no time averaging is done to reduce positional uncertainties. However, we investigated this issue by comparing the single-sample estimates of GPS position at the rapid-static sites with the computed nominal time-averaged positional solution. A typical rapid-static site with 4 minute occupation time and 5 Hz sampling rate contains 1200 single-sample estimates of GPS position. For 60 rapid-static sites, the average RMS error of the difference between the single-sample and nominal positional estimates was < 1 cm for all three coordinates (x, y, z). Thus, the accuracy of the kinematic position estimates should not be greatly affected by the lack of time averaging.

The major source of error in the kinematic data results from obstructions. Trees, buildings, and overpasses can temporarily block some or all of the available GPS satellites, thereby increasing the positional error in the kinematic data. The GPS units report a value termed the Positional

Dilution of Precision (PDOP) which is a rough estimate of the positional accuracy of the data. The GPS post-processing software uses the PDOP data and other information to provide an estimate of the total RMS error for each kinematic position. We examined the accuracy of the GPS RMS error estimates for the kinematic data by looking at the elevation residuals (differences) computed at the intersection or crossover between different traverse vectors of the survey. For perfect accuracy, the interpolated elevations at the crossing point (z_1, z_2) should be the same for each of the two traverse vectors. Thus, the RMS of the elevation residuals at these crossover points provides an estimate for the vertical accuracy of the kinematic positions. Note that uncertainties in the horizontal positions will be translated into the crossover elevation differences as well. A scatter plot of the magnitude of the elevation residuals (i.e., $| \Delta z | = | z_1 - z_2 |$) vs. the RMS error estimates from the GPS software is shown in Figure 1 for over 300 crossovers. In general, the $| \Delta z | < 10$ cm when the RMS error estimate is < 10 cm. When the RMS error estimate exceeds 10 cm, the elevation residuals can exceed several meters.

However, there exist a few points where $| \Delta z | >> 10$ cm even though the RMS error < 10 cm. Investigation of these points determined that the cause of this was due to obstructions in the recent time history of one or both of the traverse vectors. Our analysis indicates that the PDOP data and the corresponding RMS error estimates change quite dramatically over a period of only a few seconds as the survey vehicle moves in and out of obstructions. To obtain only reliable elevation estimates from the kinematic data, we developed a quality check filter to exclude data when the RMS > 10 cm. In addition, we required the RMS error to be < 10 cm for a minimum time period of 30 sec. After applying both criteria, the RMS of the crossover residuals for the two-day survey decreased to 2 cm compared to 33 cm when only the RMS < 10 cm criterion was used. To further validate this approach, we computed the crossover differences between our two-day kinematic dataset and another kinematic dataset collected in a similar survey three months later. The quality check filter was applied to both datasets prior to computing the crossover residuals. The RMS of nearly 100 crossover residuals between the two surveys was 2.5 cm. Conservatively, we believe that the RMS accuracy of the elevation estimates from the kinematic GPS data is on the order of 5-10 cm after the quality check filter is applied.

We created three different CP datasets using the quality-checked kinematic data from our two-day survey. The, CP_{K30m}, CP_{K10m}, CP_{K1m} datasets represent subsets of the overall kinematic dataset where the minimum separation between sequential positions was 30, 10, and 1 m, respectively. This is done to eliminate thousands of redundant data points created when the survey vehicle was stationary (e.g. stop light) or moving at very slow speeds. Finally, every point in each of the three kinematic datasets is cross-checked with all other points in a given dataset to eliminate redundant, non-sequential positions within the dataset that arise because of crossovers and repeat traverses along the same street. A radial search criterion corresponding to the sequential separation criterion is used for the three different datasets (i.e. R > 30, 10 or 1 m). The resulting CP_{K30m}, CP_{K10m}, CP_{K1m} datasets contain approximately 2600, 8200, and 52,000 check points, respectively.

Results and Discussion

Digital Elevation Models

After an appropriate triangulation solution is obtained, the eight digital images were processed using commercially available software for automated extraction of the digital elevation data in a grid format (PCI Geomatics, 2000). Level 0 and Level 1 DEMs were generated with horizontal resolutions of 1 m and 3 m. Figure 2 shows the 3 m Level 1 DEM in color-shaded relief format. The location of the NGS monuments (Level 0 GCPs) and the Level 1 GCPs are also shown. The DEM covers an area of roughly 185 km^2. The small areas in the far north and south that protrude out of the main part of the DEM result from the E/W stereo coverage between the two image strips (4 images/strip). The main drainage feature in the S/W, Wilson creek, is fed by four tributary creeks that originate in central portion of the city. The northenmost tributary, Jordan creek, travels through the heart of the city's urban core (J11-J12). The floodplain for the Jordan creek wathershed was recently reclassified by the Federal Emergency Management Association (FEMA) and the flooplain elevation was increased by 3 m. This placed many buildings in the downtown area within the new 100-yr floodplain, as well as a new multi-million dollar urban revitalization/greenspace corridor. A large number of urban/suburban features are clearly revealed in the 3-m DEM; these include: the urban core with multi-story buildings (J12), a railroad yard (G9), an interstate interchange (E7), shopping mall areas (L17, M7-M8), and a university campus (K12-K13). In addition, all major and minor city streets are revealed as well. The city streets take the form a N/S grid in the central area (e.g. I9, G11) and give way to more curved streets in residential areas adjacent to drainage features (e.g. F16, N17).

The 3 m Level 1 DEM was used to generate an orthorectified mosaic of the eight digital images and a grey-scale image of the surface slope. Figure 3 shows the orthoimage and slope map for the railroad yard (G9). The slope map accurately captures the footprints of the large buildings in the railroad yard as well as many of the smaller buildings in the surrounding residential/commerical areas. In addition, the portions of the railroad tracks containing boxcars are clearly revealed as well. Figure 4 shows the orthoimage and grey-scale image of the DEM for the residential area located at N17. The single-family houses and streets are clearly identifiable and conform to the major drainage feature in this area. Note that the heavily wooded areas adjacent to the drainage feature are also captured in the DEM. This is a drawback for many applications that require "bare-earth" elevations, and this problem is common among all DEMs derived from other remote-sensing techniques as well (InSAR, LIDAR, etc.). We believe that these results demonstrate that high-resolution DEMs derived from the NAPP aerial photos, and products derived thereof (slope, aspect, orthomosaic, etc.), can be effectively used for urban feature extraction, street mapping, base map registration, etc.

One of the most important application areas for high-resolution urban DEMs is for flood-plain mapping, risk assessment, and flood mitigation. Flood plain mapping and flood mitigation are critical problems in many medium-sized and larger urban areas, particularly those that are undergoing rapid urban expansion and/or change. The use of remote sensing has not been an integral part of traditional methods used by FEMA in producing 100-yr flood-plain boundaries. Traditional techniques for measuring floodplain cross-sectional elevations for hydraulic analyses are labor intensive. Consequently, only a small number of cross-sections are normally obtained to

limit costs. The smaller the number of cross-sections, the greater the uncertainty that is introduced in the computed flood elevations. In addition, the hydrologic models that provide the flow rates for the hydraulic models traditionally use lumped parameters to describe runoff characteristics that are averaged over large areas. In general, the larger the areas that are averaged, the greater the uncertainty that is introduced in the computed flow rates. High resolution DEMs can be used: a) to provide large numbers of floodplain cross-sections to improve hydraulic analyses, and b) to better define sub-basin areas and grid-cell slopes to improve hydrologic analyses. We are currently working with the City of Springfield Department of Public Works to use this high-resolution DEM along with other remote sensing data sources to assess the recent FEMA re-classification of the flood-plain boundary in the Jordan Creek watershed.

DEM Accuracy

The five check point (CP) datasets described in the previous section were used to assess the vertical accuracy of all the DEMs (Level 0 & 1, 1 m & 3 m). The RMS error (*RMSE*) is computed using

$$RMSE = \sqrt{\frac{\sum_{i=1}^{N}(Z_{icp} - Z_{idem})^2}{N-1}},$$

where Z_{icp} is the CP elevation, Z_{idem} is the DEM elevation, and N is the number of CPs. The DEM elevation is obtained from a bilinear interpolation of the four adjacent DEM grid elevations. The results are summarized in Table 2.

Table 2. *RMSE* estimates for high-resolution urban DEMs from NAPP aerial photos

DEM	*RMSE* (m) for Check Point Datasets				
	CP_{S50}	CP_{S100}	CP_{K30m}	CP_{K10m}	CP_{K1m}
Level 0 - 1 m	1.80	2.23	2.79	2.95	2.93
Level 0 - 3 m	1.82	2.66	2.48	2.42	2.31
Level 1 - 1 m	1.11	2.11	2.28	2.58	2.40
Level 1 - 3 m	1.03	1.43	1.85	1.81	1.70

The results show that the *RMSE* varies between 1-3 m for the various DEMs and CP datasets. However, the low end of this range is overly optimistic because it is obtained for the Level 1 DEMs using the CP_{S50} dataset. These points were selected *a priori* for sharp and distinct point features. Thus, the stereo-correlation errors should be a minimum at these points and therefore underestimate the true *RMSE*. Since the three kinematic CP datasets (CP_{K30m}, CP_{K10m}, & CP_{K1m}) contain many thousands of spatially distributed CPs, we believe they provide the best overall estimates for the *RMSE*. The *RMSE* estimates from the kinematic datasets generally agree to within about 0.15 m for most of the DEMs. Thus, it appears that the finer spacing and much larger number of CPs in the CP_{K1m} dataset offers no significant advantage in characterizing the *RMSE* for the DEMs in this study. The *RMSE* estimates from the CP_{S100} dataset are substantially different than those from the

kinematic CP datasets. This suggests that 100 CPs is insufficient to characterize the overall *RMSE* for these DEMs. Note that the CP_{S100} dataset was provided from an independent source, and these points were never utilized as GCPs. A good discussion of the effect of sample size on DEM error estimates can be found in Li (1991). Following Li's analysis, the theoretical reliability of the *RMSE* estimates is about 7% for a sample size of 100. However, the results in Table 2 show that the difference between the *RMSE* estimates from the CP_{S100} and CP_{K1m} datasets averages around 15%. Similarly, the differences of the *RMSE* estimates among the three kinematic CP datasets due to sample size variations is much larger than that predicted by theory. This suggests that the variability of the *RMSE* estimates is also significantly affected by the spatial distribution of the CP data. Nevertheless, the results in Table 2 for the kinematic CP datasets indicate that the *RMSE* estimates are accurate to better than 10%.

The *RMSE* estimates for the Level 1 DEMs are about 0.5 m lower than the *RMSE* estimates of the Level 0 DEMs for the same xy resolution. This is clearly due to the large difference between the number of GCPs used in the triangulation solutions for the Level 0 vs. Level 1 DEMs (i.e., 8 vs. 46 GCPs). Figure 5 shows a plot of the *RMSE* vs. the number of GCPs for a 3 m DEM. The CP_{K30m} and $_{CPK10m}$ datasets were used to estimate the *RMSE* and the rapid-static GCPs were used for all triangulation solutions. For each triangulation solution, we selected each set of GCPs such that they were uniformly distributed throughout the study area. The results indicate that there is virtually no benefit gained in terms of a reduced *RMSE* when using more than about 25 GCPs for the 3-m DEM. Thus, it would seem that uniform GCP distribution is more important than obtaining a large number of GCPs. These results also suggest that about 3 GCPs per photo is sufficient to obtain the best possible vertical accuracy for high-resolution DEMs derived from NAPP photos.

The *RMSE* estimates for the 1 m DEMs are about 0.5 m larger than for the corresponding 3 m DEMs with the same number of GCPs (i.e., Level 0 vs. Level 1). Visual comparison of the 1 m and 3 m DEMs indicates that there is only a small improvement in the ability to discriminate small-scale features. This improvement is much smaller than what is implied by the three-fold reduction in the horizontal resolution, and a ~30% increase in the *RMSE* is the tradeoff for this small improvement. This occurs because it becomes increasingly more difficult for automated stereo-correlation algorithms to precisely match pixel locations in stereo images as the DEM xy resolution approaches the pixel resolution of the image. For a 1 m DEM and a 0.85 m pixel resolution, the stereo-correlation algorithm must be able to match each pixel in a given image with the corresponding pixel in the stereo pair. For a lower resolution DEM, the matching is done using a cluster of pixels. Thus, it is reasonable to expect that stereo-correlation errors will increase the random error in DEMs where the xy resolution approaches that of the image resolution. This is consistent with the results in Table 2. We note that in some applications (e.g. feature extraction), the increase in DEM error may be an acceptable tradeoff for obtaining a modest improvement in the ability to resolve fine-scale features.

DEM Resolution, Accuracy, and Cost

The *RMSE* for the 3 m Level 1 DEM is on the order of 1.8 m. Relative to the USGS Level 1 DEMs derived from the same NAPP photography, this is a ten-fold improvement in horizontal (xy) resolution and a reduction in RMS vertical (z) accuracy by a factor of four to eight. In addition, the

xy resolution and z accuracy are both many times better than the highest resolution/highest accuracy DEMs derived from current optical and radar satellite systems. Compared to current airborne InSAR systems, the xy resolution is several times better while achieving comparable z accuracy (e.g. Intermap, 2000). Compared to current airborne LIDAR systems, the xy resolution is comparable but the z accuracy is several times larger (e.g. Terrapoint, 2000).

The approach outlined here has two main advantages relative to commercial airborne InSAR and LIDAR systems. First, the NAPP data are currently available for about 95% of the continental U.S. Thus, the NAPP data are an existing and widely available data source that can be used by anyone wishing to develop high-resolution DEMs for any application, urban or otherwise. Second, and most important, the cost of the NAPP data for this study, including precision scanning, was a few hundred dollars. This is several orders of magnitude smaller than what it would cost to acquire commercial InSAR and LIDAR datasets for a similarly-sized area. Thus, the NAPP data are a viable, low cost, data source that can be used to provide high-resolution DEMs for small and medium sized city and county governments. While we utilized precision GPS to provide our GCP datasets, traditional land survey methods could also be used to provide the necessary GCPs. Moreover, GPS surveying is finding widespread adoption even in smaller cities, and we note that the City of Springfield has had this capability for several years. The costs of computer hardware and commercial software needed to produce the high-resolution DEMs are one-time expenses. If included in the cost of the DEM, the total cost would still be significantly less than the current cost of other commerical high-resolution DEMs. Moreover, we believe that private-sector service companies could easily incorporate this approach and spread these one-time costs over many customers. This could make high-resolution/high-accuracy DEMs available to smaller cities and counties who would otherwise be unable to afford more expensive commercial datasets.

Conclusions

This paper demonstrated that 1:40,000-scale NAPP aerial photos, digitally scanned at 21.2 μm and processed using commercially available stereo-correlation software, can be used to produce DEMs of sufficient resolution and accuracy to be useful in many urban-area applications. We generated DEMs with a 1 m and 3 m horizontal resolution for the medium-sized city of Springfield, Missouri using variable amounts of ground control. The results showed that very fine-scale urban and suburban features (buildings, streets, etc.) could be easily resolved in the DEMs. Analysis of the DEMs using a database of more than 50,000 check points derived from a kinematic GPS survey indicated that RMS vertical accuracies of ~ 1.8 m can be obtained. This level of accuracy required about 25 ground control points (GCPs) that were uniformly distributed throughout the study area (≈ 3 GCPs/photo).

Both the horizontal resolution and vertical accuracy of the DEMs generated in this study are many times better than that currently available from optical or radar satellite remote sensing systems. In addition, the NAPP imagery represent an inexpensive data source that is readily available throughout most of the continental U.S. The exploitation of the NAPP data could make high-resolution/high-accuracy DEMs available to smaller cities and counties who would otherwise be unable to afford more expensive commercial datasets of comparable resolution and accuracy.

Acknowledgements

We wish to thank Dan Daugherty for the DEM visualizations, Joe Engeln and Hal Johnson for assistance in the GPS survey, and Jack Dill and the City of Springfield for providing the additional GPS-surveyed check points. This work was supported by NASA/Stennis Space Center under Grant No. NAG13-99014.

References

Al-Rousan, N., P. Cheng, G. Petrie, Th. Toutin, and M.J. Valadan Zoej, 1997, Automated DEM Extraction and Orthoimage Generation from SPOT Level 1B Imagery, *Photogrammetric Engineering & Remote Sensing*, 63(8):965-974.

Fukushima, Y., 1988, Generation of DTM Using SPOT Image Near Mt. Fuji by Digital Image Correlation, *Intl. Archives of Photogram. and Remote Sensing*, 27(B3):225-234.

Gens, R. and J. Van Genderen, 1996, SAR Interferometry – Issues, Techniques, Applications, *International Journal of Remote Sensing*, 17:1803-1835.

Intermap, Inc., 2000, http://www/digitalglobe.com

Li, Z., 1991, Effects of Check Points on the Reliability of DTM Accuracy Estimates Obtained from Experimental Tests, *Photogrammetric Engineering & Remote Sensing*, 57(10):1333-1340.

Light, D.L., 1993. The National Aerial Photography Program as a Geographic Information System Resource, *Photogrammetric Engineering & Remote Sensing*, 59(1):61-65.

NASA Shuttle Radar Topography Mission, 2000, http://www.jpl.nasa.gov/srtm

PCI Geomatics, 2000, OrthoEngine Airphoto DEM.

Rodriguez, V., P. Gigord, A.C. de Gaujac, P. Munier, and G. Begni, 1988, Evaluation of the Stereoscopic Accuracy of the SPOT satellite, *Photogrammetric Engineering & Remote Sensing*, 54(2):217-221.

Rufino, G., A. Moccia, and S. Esposito, 1998, DEM Generation by Means of ERS Tandem Data, *IEEE Transactions on Geoscience and Remote Sensing*, 36(6):1905-1912.

Sasowksy, K.C, G.W. Peterson, and B.M. Evans, 1992, Accuracy of SPOT Digital Elevation Model and Derivatives: Utility for Alaska's North Slope, *Photogrammetric Engineering & Remote Sensing*, 58(6):815-824.

SPOT Image Inc., 2000, http://www.spot.com

Terrapoint Inc., 2000, http://www.terrapoint.com

United States Geological Survey, 1997. Standards for Digital Elevation Models, Part 1: General; Part 2: Specifications; Part 3: Quality Control, Department of the Interior, Washington, DC.

List of Figures

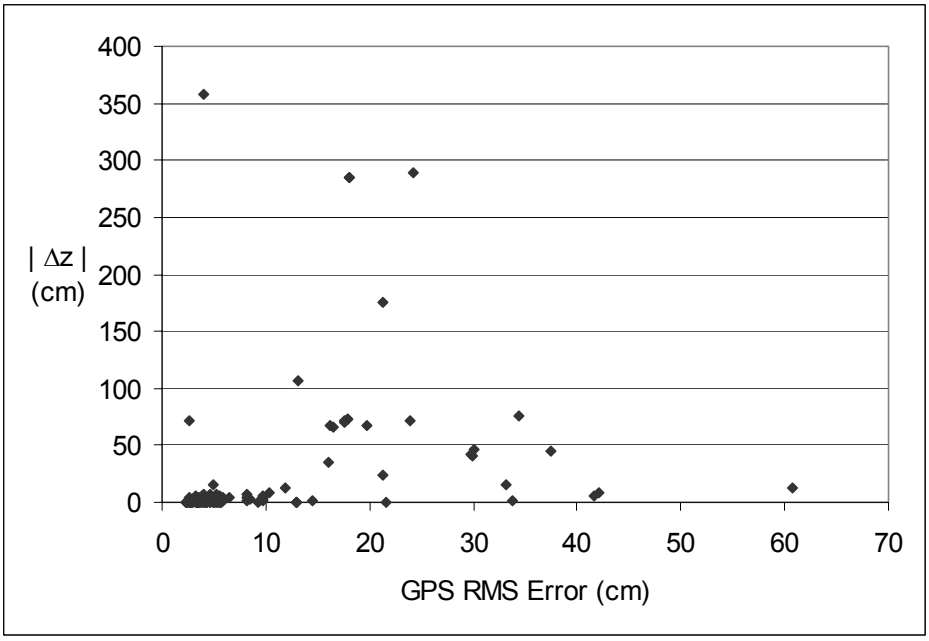

Figure 1. Comparison of elevation differences at crossover points of kinematic GPS survey vectors and the corresponding RMS error estimates from GPS post-processing software.

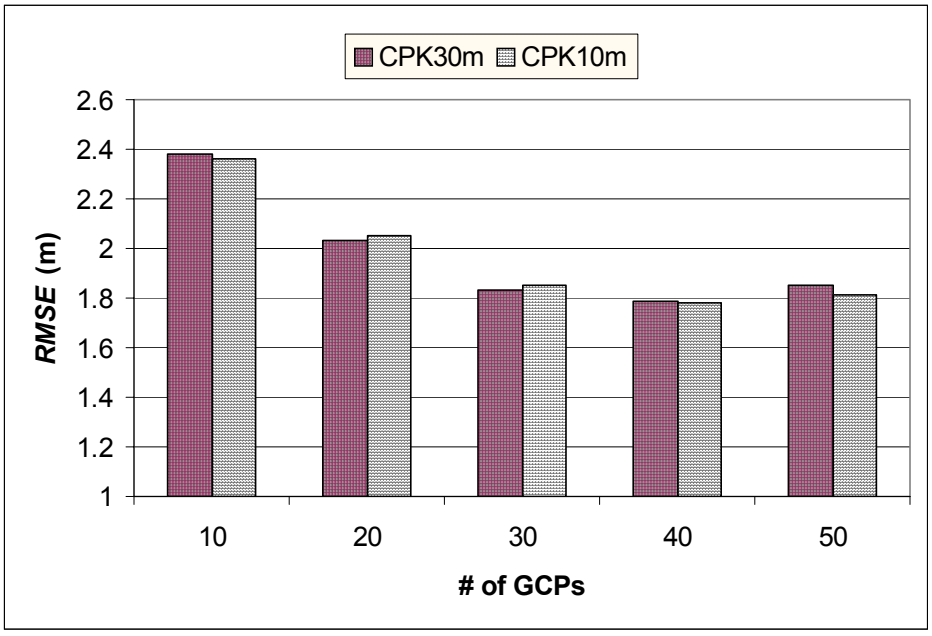

Figure 5. Comparison of estimated error (*RMSE*) vs. the number of Ground Control Points (GCPs) used in the triangulation solution for a 3 m horizontal resolution DEM.